Electrochemical Iron Recovery from Biologically Produced Magnetite via Iron Oxide/Hydroxide Conversion: First Steps towards Terrestrial and Martian Applications

Reza Fayaz[1,5,6], Antoine Carissimo[3,5,6], Md Izzuddin Jundullah Hanafi[4,5], Guillaume Pillot[3,5,6], Michael Baune[1,6], Thorsten M. Gesing[4,5], Sven Kerzenmacher[3,5,6], Fabio La Mantia[2,5,6] & Jorg Thöming[1,5,6]*

[1]University of Bremen, Chemical Process Engineering Group (CVT), Leobener Strasse 6, 28359 Bremen, Germany
[2]University of Bremen, Energy Storage and Conversion Systems, Wiener Strasse 12, 28359 Bremen, Germany
[3]University of Bremen, Environmental Process Engineering Group (UVT), Leobener Strasse 6, 28359 Bremen, Germany
[4]University of Bremen, Institute of Inorganic Chemistry and Crystallography, Leobener Strasse 7, 28359 Bremen, Germany
[5]University of Bremen, MAPEX Center for Materials and Processes, Bibliothekstrasse 1, 28359 Bremen, Germany
[6]University of Bremen, Center for Environmental Research and Sustainable Technology (UFT), Leobener Strasse 6, 28359 Bremen, Germany
*Email: thoeming@uni-bremen.de

ABSTRACT

Ferrihydrite ($Fe_{10}O_{14}(OH)_2$), an iron oxide/hydroxide, is found in a variety of terrestrial and interplanetary environments. This study presents a novel combination of bio-mineralization and electrolysis to address the need for efficient mining of low-grade iron resources. Iron-reducing bacteria biologically convert iron oxide/hydroxide to magnetite. This could then be magnetically extracted and electrolyzed at 363 K using an alkaline medium into metallic iron. The innovation could facilitate the exploitation of marginal iron reserves, particularly in areas where no rich ores are available. The process also promises adaptation to extraterrestrial sources such as the Martian regolith.

In our research, *Carboxydothermus ferrireducens* converted superparamagnetic iron oxide/hydroxide (Fe(III)) into a ferrimagnetic (Fe(II)/Fe(III)) phase. After 20 hours of alkaline deoxidation electrolysis, this 'bio-magnetite' could be electrochemically reduced to 25 wt.% of Fe(0). The iron yield was increased to 67 % by integrating a heat treatment step. This resulted in a high current efficiency of 63 % and an energy consumption of 17.9 MJ/kg, competitive with current industrial practices. The morphological and chemical changes induced by heat treatment facilitated iron reduction and minimized parasitic hydrogen evolution. Improved reducibility of bio-mineralized materials was also observed. These findings suggest the potential of biotechnological approaches in metallurgy.

1. Introduction

Metallic iron, Fe(0), is a valuable material globally, and its demand is expected to continue to rise [1]. The traditional process of smelting iron with coke produces significant emissions of greenhouse gases and a high turnover of energy [2], so finding environmentally friendly alternatives is crucial [3]. While hydrogen is widely used for direct iron reduction processes [4], electrochemical reduction has also been proposed to replace current polluting methods [5,6,7]. However, most efforts to date have concentrated on high-value resources, and innovations that can utilize currently unusable iron resources may have significant economic and strategic implications in the future.

Especially for such currently unusable iron resources like low-grade ores, traditional iron extraction methods pose challenges to the Sustainable Development Goals (SDGs) [8], including SDG 13 (Climate Action) and SDG 7 (Affordable and Clean Energy). Based on the utilization of renewable energy and electrochemistry to support SDG 12 (Responsible Production) [9], this paper presents a concept for converting low-grade iron ore (bio-) electrochemically into iron. This concept also offers the possibility of extracting iron on Mars using locally available materials and renewable energy sources. Thereby, it complements established in-situ resource utilization (ISRU) methods, such as MOXIE [10], which produces oxygen from CO_2 on Mars.

Ferrihydrite, an iron oxide/hydroxide with variable iron content, occurs predominantly as an

amorphous phase in sands, sediments, and laterites [11]. It is also a major component of Fe-rich sludges derived from water treatment plants and mining and ore processing industries [12]. This iron oxide/hydroxide is not normally targeted for iron extraction due to its amorphous nature and association with various impurities. Given the future depletion of high-grade iron ore reserves, alternative approaches are being sought to convert low-grade ores into useful products. The bio-mineralization of these underutilized resources could play a role in their future use [13].

In addition, iron fabrication using ISRU-generated electricity as the power source is crucial for future Mars exploration and habitation [14,15]. Martian regolith contains several metal oxides, including iron-bearing phases like ferrihydrite [16], but its complex mineralogy makes direct electrolysis challenging. Current methods, such as molten regolith electrolysis (MRE), operate at extreme temperatures (~1873 K) and result in partial reductions and mixed metallic mixtures [17,18]. Solid-state reduction at relatively lower temperatures (~1173 K) also struggles with incomplete oxygen removal and unselective metal extraction [19]. Given these limitations, pre-concentrating iron oxides from regolith would simplify the process and enable more efficient, lower-temperature electrolysis, reducing complexity and energy requirements.

Iron oxides exhibit semiconducting properties, making direct electroreduction challenging [20]. However, solid-state deoxidation electrolysis of hematite [5] and magnetite [21] has been successfully achieved in an aqueous medium at a moderate temperature of 363 K. A study [22] indicated that hematite displays higher reducibility and current efficiency in electrochemical reduction compared to magnetite, which suffers from slower reduction kinetics and lower efficiency due to side reactions such as hydrogen evolution. In this process, iron oxides are reduced to metallic iron in an electrolytic cell. A pure iron oxide pellet is the cathode, submerged in a highly alkaline solution. During the reduction, iron ions are converted to metallic iron at the cathode, while oxygen ions are expelled and migrate to the anode, where they are released as oxygen gas [6,7].

However, this electrochemical process is sensitive to impurities in the feedstock. Studies on $Fe_{2.3}Mg_{0.7}O_4$ spinel [23], red mud [24], and pseudobrookite (Fe_2TiO_5) [25] have shown that impurities such as Mg, Si, Al, and Ti significantly hinder the efficiency of the process by blocking electrochemical active sites and reducing current efficiency of any ionic iron species. These findings highlight the detrimental effects of impurities on direct electroreduction. To address this challenge, this research explores bio-mineralization as a pre-treatment method. The biological conversion of ferric oxide to magnetically responsive forms allows selective concentration of iron and separation of impurities before electrolysis, thereby mitigating the negative effects of impurities and improving process efficiency.

Bio-mining uses biological systems, usually microorganisms, to extract and recover valuable metals from ores and waste materials [26]. It holds the potential for ISRU, but the technology is still in its infancy [27]. A series of biomining experiments conducted on board the International Space Station (ISS) demonstrate that the process is effective regardless of gravity conditions [28]. Recently, a novel biomining approach based on bio-mineralization and magnetic extraction has been conceptualized and evaluated as promising [29]. It relies on the ability of iron-reducing microorganisms to bio-mineralize magnetite during the reduction of ferric iron oxides, a naturally occurring process in sediments [13]. To the best of our knowledge, this biomineralization approach has only been experimentally tested once with Martian and Lunar simulants, leading to a significantly increased iron extraction, thereby highlighting its potential for ISRU [30]. However, this biological process does not convert the iron to Fe(0).

In this study, we demonstrate the advantage of bio-mineralization in potentially enriching low-grade iron ores to make them more suitable for electrochemical reduction. First, iron-reducing bacteria convert iron-bearing phases into magnetically responsive bio-magnetite. The bio-mineralization Fe(II)/Fe(III) mineral is then reduced to Fe(0) by electrolysis. An intermediate heat treatment step is introduced to increase iron yield further and reduce energy consumption.

The improved reducibility of bio-mineralized materials suggests a promising route for economically viable iron extraction. This approach also offers a practical solution for extraterrestrial environments such as Mars, where conventional extraction methods are not feasible.

2. Materials and methods

2.1. Bio-mineralization

The iron oxide/hydroxide was prepared by gradually adding NaOH 10 M in a solution of $FeCl_3 \cdot H_2O$ (108 g/L) until the pH stabilized at 7. The iron oxide/hydroxide suspension was then centrifuged and washed with deionized water.

Bio-magnetite was prepared by providing this iron oxide/hydroxide to *Carboxydothermus ferrireducens*, an iron-reducing bacterium, as the terminal electron acceptor for anaerobic respiration. *C. ferrireducens* was purchased from DSMZ (DSM 11255). It is a thermophile (323 to 347 K) and a facultative autotroph, isolated from hot springs in Yellowstone National Park, Wyoming, USA. To simplify cultivation, the bacterium was cultivated organoheterotrophically with glycerol as the carbon and energy source. It was cultivated anaerobically in 1 L Schott bottles.

The medium contained, per liter of deionized water: 0.33 g of KH_2PO_4, 0.33 g of NH_4Cl, 0.33 g of KCl, 0.33 g of $MgCl_2 \cdot 6H_2O$, 0.33 g of $CaCl_2 \cdot 2H_2O$, 0.2 g of $MgSO_4 \cdot 7H_2O$, 2.5 g of $NaHCO_3$, 0.1 g of yeast extract, and 1 mL of Wolfe's mineral elixir (trace elements solution, DSMZ). All chemicals were > 99 % pure and purchased from Carl Roth (Germany), Merck (Germany), or VWR International (United States). The medium was prepared in an anaerobic chamber, adjusted to pH 6.8 with 1 M HCl, and autoclaved. $CaCl_2 \cdot 2H_2O$ was added to the medium after autoclaving, from an autoclaved concentrated solution. The trace elements solution contained, per liter of deionized water: 30 g of $MgSO_4 \cdot 7H_2O$, 5 g of $MnSO_4 \cdot nH_2O$, 10 g of NaCl, 1 g of $FeSO_4 \cdot 7H_2O$, 1.8 g of $CoCl_2 \cdot 6\ H_2O$, 1 g of $CaCl_2 \cdot 2H_2O$, 1.8 g of $ZnSO_4 \cdot 7H_2O$, 0.1 g of $CuSO_4 \cdot 5H_2O$, 0.18 g of $AlK(SO_4)_2 \cdot 12H_2O$, 0.1 g of H_3BO_3, 0.1 g of $Na_2MoO_4 \cdot 2H_2O$, 2.8 g of $(NH_4)_2Ni(SO_4)_2 \cdot 6\ H_2O$, 0.1 g of $Na_2WO_4.2H_2O$, and 0.1 g of Na_2SeO_4. The salts were dissolved after adjusting the pH to 1.0 with sulfuric acid. The medium was distributed to three 1 L cultivation bottles containing 500 mL of medium. After autoclaving, the cultivation bottles were complemented with glycerol (40 mM), iron oxide/hydroxide (100 mM of Fe^{3+}), and $Na_2S \cdot 9H_2O$ (0.05 mM of Na_2S) from concentrated solutions. The glycerol-concentrated solution was autoclaved while the $Na_2S \cdot 9H_2O$ solution was filter-sterilized. Iron oxide/hydroxide was not autoclaved to prevent crystallization. The cultivation bottles were inoculated with 8 mL of iron oxide/hydroxide-reducing *Carboxydothermus* cultures, and placed in an incubator (Heratherm, Thermo Fisher Scientific, USA) at 338 K and magnetically stirred at 400 rpm for about 48 h until the particles in the medium became black and magnetic. The concentration of Fe^{2+} was measured spectrophotometrically with the ferrozine assay [31]. Before measurements, 1 mL of the sample was mixed with 1 mL of 4 M HCl until the particles were visually dissolved (less than an hour to a few days for the final samples with black magnetic particles). Cells were observed during cultivation under a fluorescence microscope. Liquid samples were stained with 2 µg/mL of 4′,6-diamidine-2-phenylindole (DAPI) (Carl Roth, Germany), illuminated with ultraviolet light (385 nm), and observed with a Zeiss Microscope Axioscope 7 (Carl Zeiss, Germany) at 500x magnification (reflected light at 465 nm). At the end of cultivation, the magnetic particles were rinsed with deionized water once and dried at room temperature. In total, about 14 g of black magnetic particles were obtained from the 3 cultures.

2.2. Sample Preparation

The heat treatment was done under air at 1173 K for 3 h. The commercial materials used were hematite powder (Carl Roth, ≥ 95 %, 400 mesh) and magnetite powder (Thermo Scientific, ≥

97 %, 325 mesh). An electrolyte solution was prepared by dissolving 10 M NaOH (VWR, 99.3 %) in water. This highly concentrated electrolyte solution should minimize hydrogen evolution reaction (HER) and reduce water loss [32]. A Martian regolith simulant, MGS-1 (Space Resource Technologies (SRT), batch code: 002-05-001-0621, mean particle size: 90 μm) was analyzed to understand the mineral composition and identify the iron-containing phases. For cathode pellet formation a conductive Ag-paste (MG Chemicals, product code: 8330S-A) was used for pelletization to replace the commonly used sintering, which causes mineral phase alteration of precursors. Approximately 1 g of powder was used to produce each disk-shaped pellet (diameter: 10 mm, thickness: 3 mm). Around 2 mL of glue was applied to each pellet, and cured at 353 K for 2 h.

To account for the potential effect of silver epoxy on the electrochemical measurements, electrolysis was performed using samples containing only Ag paste. Initially, it was confirmed that silver was not involved in the electrochemical reaction, as no phase change was observed post-electrolysis (confirmed by X-ray powder diffraction (XRPD) analysis). The charge resulting from this control experiment was measured (2420 C for 20 h) and subtracted from the total electrical charge obtained from the main electrolysis experiments. This ensured that the HER associated with silver was excluded from the calculations.

2.3. Electrochemical experiments

Electrical contacts were established by connecting a Kanthal® wire to a hole in the center of the cathode pellet. An anion exchange membrane (Reichelt Chemietechnik, MA-3475) was employed to separate the electrodes. Before each test, the membrane was activated by immersing it in a 10 % salt solution at 328 K for 3 h. The electrochemical tests were conducted in a Teflon H-cell separated by an anion exchange membrane (AEM). The working electrode consisted of iron oxide/hydroxide, bio-magnetite, bio-hematite, commercial magnetite, or commercial hematite pellets connected to the wire. A reference electrode of Ag|AgCl|KCl (3.5 M) with a potential of +0.205 V vs. the standard hydrogen electrode (Xylem Analytics) was utilized. Based on insights from our prior study [5], we employed Ni/Fe as a non-contaminating inert counter electrode, which also catalyzes oxygen evolution and reduces the anodic overpotential [33]. This anode electrode was a rod-shaped Ni36/Fe64 alloy, with a diameter of 20 mm and a height of 100 mm. The measurement equipment employed was a potentiostat (IPS Elektroniklabor, PGU-1A-OEM). Before conducting electrochemical tests, the cathode electrodes were immersed in the electrolyte (10 M NaOH with a pH of 15) for 30 minutes to ensure proper wetting.

To screen electrochemical redox peaks at the hematite/electrolyte interface, cyclovoltammetry (CV) tests were performed. The CVs were recorded with a scan rate of 50 mV/s, within a range of 1.8 V to +0.5 V relative to the open circuit potential. They were repeated for 3 cycles. Electrolysis tests (chronoamperometry) were conducted by applying a constant potential of -1.4 V vs. the Ag/AgCl reference electrode for 20 or 5 h while measuring the corresponding current. A second potentiostat (IPS Elektroniklabor, IMP 83 PC T-BC) was employed to measure the total cell voltage during electrolysis for the sake of energy calculations. All electrochemical tests were conducted in an argon-protected atmosphere to suppress the carbon parasitic reaction loop [5].

2.4. Sample characterization

After the reduction process, the electrodes were pulled above the electrolyte line and dried under argon. They were pulled out after the cell cooled. To eliminate any residual electrolyte, the cathode samples were subjected to Soxhlet extraction with water as the solvent for up to 5 h [34]. Subsequently, the samples were dried in an oven at 80 °C for 1 h and weighed. To characterize the samples, they were ground and subjected to XRPD analysis [35]. XRPD measurements were carried out on a Bruker D8 Discover diffractometer using CuKα1,2

radiation ($\lambda_{K\alpha1}$ = 154.05929(5) pm, $\lambda_{K\alpha2}$ = 154.4414(2) pm) in Bragg-Brentano geometry. Data was collected at ambient conditions in a range of 20° to 100° 2θ, with a step width of 0.0149° 2θ and a measurement time of 0.3 seconds per step using an energy-discriminating LynxEye-XET multi-strip detector. The Rietveld refinements were performed using TOPAS V6.0 (Bruker AXS). The average crystallite size of the amorphous scattering samples was determined using the EnvACS approach [36]. For elemental mapping of selected sponges produced, scanning electron microscopy (SEM, Device: JEOL, JMS-6510) and energy dispersive X-ray spectrometer (EDX, Device: Bruker, XFlash 410-M) analyses were performed. The specific surface area of the sample was measured using a Brunauer-Emmett-Teller (BET) surface area analyzer, Belsorb Mini (Microtrac), with N_2 as an adsorption gas. Samples were pre-treated at 393 K for 3 h in a vacuum.

3. Results and discussion

Ferrihydrite, an iron-rich component of various natural soils, industrial wastes, and Martian regolith, is classified as iron oxide/hydroxide. In this study, we synthesized a chemically similar compound to serve as the starting material. This compound was selected for its ability to support microbial respiration under anoxic conditions. Due to the variable iron content and amorphous nature of ferrihydrite, we could not confidently confirm the identity of our synthesized material as ferrihydrite. We referred to it instead as 'iron oxide/hydroxide'.

Bio-magnetite was produced by supplying this iron oxide/hydroxide to the iron-reducing bacterium *C. ferrireducens* as the terminal electron acceptor for anaerobic respiration. That is, the synthesized iron oxide/hydroxide was included in the cultivation medium of *C. ferrireducens*, which couples the oxidation of glycerol with the reduction of ferric iron oxide/hydroxide to support its metabolism (anaerobic respiration) [37]. Upon reduction of the Fe(III) cations into Fe(II), the iron oxide/hydroxide was transformed into magnetite, a mixed-valent mineral. The concentration of Fe(II), measured spectrophotometrically after extraction in HCl, increased over time, reaching about 35 % of Fe(III) reduction after two days of cultivation (Figure 1a). A black magnetic material was formed and identified as magnetite using X-ray powder Bragg-Rietveld (XRPD) data (Supplementary S2). Microbial cells were observed at the surface of the particles (Figure 1b), with error bars based on three independent replications of the experiment. These results align with what was previously reported for this iron-reducing species [37,38].

In this study, glycerol was used as a carbon and energy source for bacterial cultivation. On Mars, however, organic carbon could be produced using cyanobacteria, which fix carbon from CO_2 without relying on carbohydrate feedstocks [39,40]. Additionally, some (hyper)thermophilic iron-reducing microorganisms (IRM), including *C. ferrireducens* [41], can function as facultative lithoautotrophs [42], utilizing only inorganic sources like H_2 and CO_2, making them suitable for cultivation without organic carbon.

Magnetite bio-mineralization by IRM typically occurs at circumneutral pH levels, around 7, where these neutrophilic microorganisms thrive. They can grow and reduce iron across a wide temperature range, from -2°C to 121°C [43,44], and are categorized as psychrophiles, mesophiles, thermophiles, or hyperthermophiles based on their optimal growth temperatures. In this study, the thermophilic bacterium *C. ferrireducens* was used, which grows optimally at 65 °C and within a pH range of 5.5 to 7.6 [37]. These properties make *C. ferrireducens* particularly suitable for bio-mining processes that demand robust microorganisms capable of thriving in diverse and extreme environmental conditions.

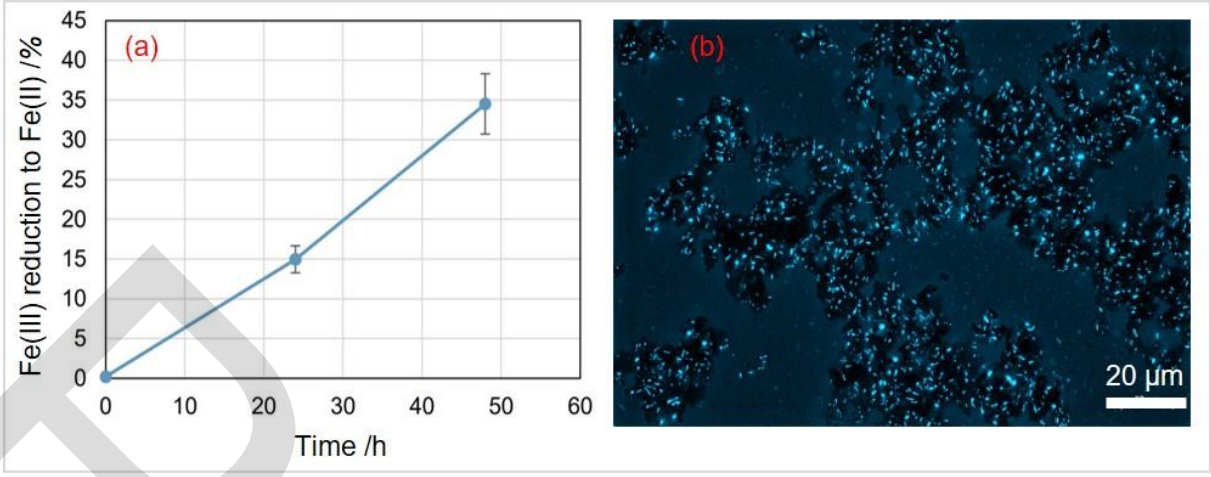

Figure 1. Growth of the iron-reducing bacterium with iron oxide/hydroxide. (a) The ratio of Fe(II) produced to the initial Fe(III) concentration, as a function of time. The average for three cultures is shown, with error bars indicating the standard deviation. (b) Black magnetic particles from *C. ferrireducens* cultures (2 days) were observed with fluorescent light, revealing the presence of microbial cells (blue) all over the particles.

The process diagram (Figure 2) illustrates the preparation of three different iron-based materials for alkaline electrolysis. It begins with iron oxide/hydroxide, which undergoes bio-mining to produce bio-magnetite. This bio-magnetite can either be used directly or further processed through heat treatment (1173 K, 3 h, under air) to examine the effects of chemical and microstructural alterations on electrochemical behavior. All three materials, iron oxide/hydroxide, bio-magnetite, and the heat-treated product, are then pelletized. These pellets serve as cathodes in an alkaline electrolysis setup operating with a 10 M NaOH solution at 363 K. Each pellet undergoes cathodic reduction at -1.4 V vs. Ag/AgCl for conversion to Fe(0). X-ray powder diffraction refinements (Supplementary S2) and Brunauer-Emmett-Teller (BET) analyses revealed changes in the crystal structure induced by bio-mining and heat treatment. Bio-mining reduced the specific surface area (SSA) from 285 m^2/g for the iron oxide/hydroxide to 41.5 m^2/g for bio-magnetite. XRPD data also confirm that bio-mining successfully converted a quantum-crystalline iron oxide/hydroxide with an average crystallite size (ACS) of 2.7(1) nm into a micro-crystalline bio-magnetite with an ACS of 16.2(2) nm (Table 1). Due to its high diffuse scattering content, the ACS of iron oxide/hydroxide could only be determined using the PDF EnvACS method [36] (Supplementary S3). This transformation can be explained by bacterial metabolic activities so that bacterial structures such as cell walls, membranes, or debris act as nucleation points for crystallization [45,46].

XRPD also confirmed the full oxidation of bio-magnetite (Fe(II)/Fe(III)) to a single (Fe(III)) phase ('bio-hematite') via heat treatment. The heat consumes the oxygen released from the bio-magnetite during the bio-mineralization phase. Following this, the SSA further declined to 0.27 m^2/g for bio-hematite, accompanied by an increase in the degree of crystallinity (DC) to 96(5) % and the ACS to 238(6) nm). The numbers in brackets represent the estimated standard deviations of the obtained values in the last digit.

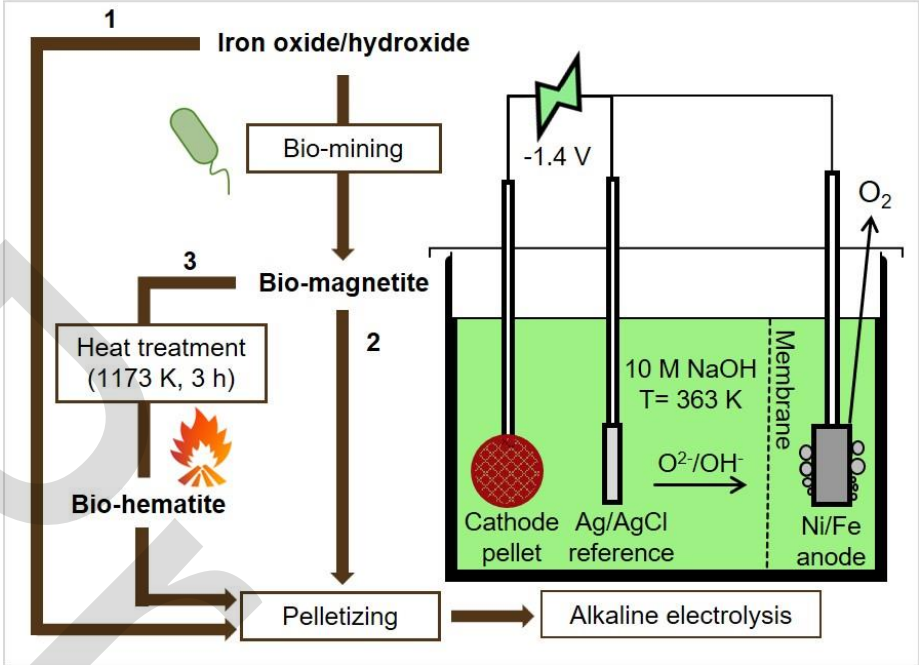

Figure 2. Schematic diagram showing the production process of bio-magnetite from iron oxide/hydroxide, followed by pelletizing with optional heat treatment. The pellets are then used in alkaline electrolysis for electrochemical conversion to Fe(0) at 363 K. Electrolysis is conducted in a two-compartment cell separated by an anion exchange membrane. The cathode pellets are then subjected to characterization analyses.

Table 1. The degree of crystallinity (DC), average crystallite size (ACS), and specific surface area (SSA) of the various feedstocks. The numbers in brackets are the estimated standard deviations of the obtained values in the last digit. (*) XRPD data of iron oxide/hydroxide shows broad humps associated with the quantum-crystalline phase which makes it impossible to distinguish the amorphous content.

Sample	DC /wt.%	ACS /nm	SSA /(m^2/g)
Iron oxide/hydroxide	*	2.7(1)	285
Bio-magnetite	80(5)	16.2(2)	41.5
Commercial magnetite	87(5)	74(1)	8.1
Bio-hematite	96(5)	238(6)	0.27
Commercial hematite	95(5)	135(1)	2.6
Heat-treated commercial hematite	99(5)	173(2)	0.76

3.1. Comparative electrochemical analysis

To observe the changes caused by bio-mining and heat treatment on the electrochemical process of iron reduction, CV and chronoamperometry tests were conducted for the starting iron oxide/hydroxide, bio-magnetite, and bio-hematite.

In the first CV cycles, the plots for the three materials tested are superimposed, with no discernible redox peaks (Supplementary S4), indicating that the iron oxide surfaces had not yet

reached electrochemical activity. This initial lack of activity is consistent with the need for surface conditioning, where repeated cycling activates the material and enhances electron transfer. However, clear electrochemical behavior is apparent in the third CV cycle (Figure 3a). The cathodic current peak at approximately -1.3 V vs. Ag/AgCl reference electrode is attributed to iron reduction. For iron oxide/hydroxide and bio-magnetite, reduction peaks start earlier than bio-hematite and show higher cathodic currents. The parasitic HER starts in all samples shortly after the reduction peak of Fe(0) formation. However, the onset of HER shows higher cathodic currents in bio-magnetite and the highest currents in iron oxide/hydroxide.

In addition, whereas there is a more pronounced boundary between the iron and HER peaks for bio-hematite, these appear to be more disruptive for iron oxide/hydroxide and bio-magnetite. During the anodic sweep, the corresponding anodic currents are higher for bio-magnetite, possibly due to high capacitive currents [47] or more likely due to superimposed Faradaic currents such as the re-oxidation of hydrogen potentially trapped in the microstructure.

Consequently, electrolysis tests were conducted by applying a potential of -1.4 V vs. Ag/AgCl for 20 h. It should be noted that the application of a potential of -1.3 V vs. Ag/AgCl did not result in any reduction of iron cations. Likely, overcompensation for the mass transfer resistance caused by limiting diffusion in boundary layers is required. The corresponding electrolysis currents were measured over time (Figure 3b) and the iron extraction yields were determined via XRPD.

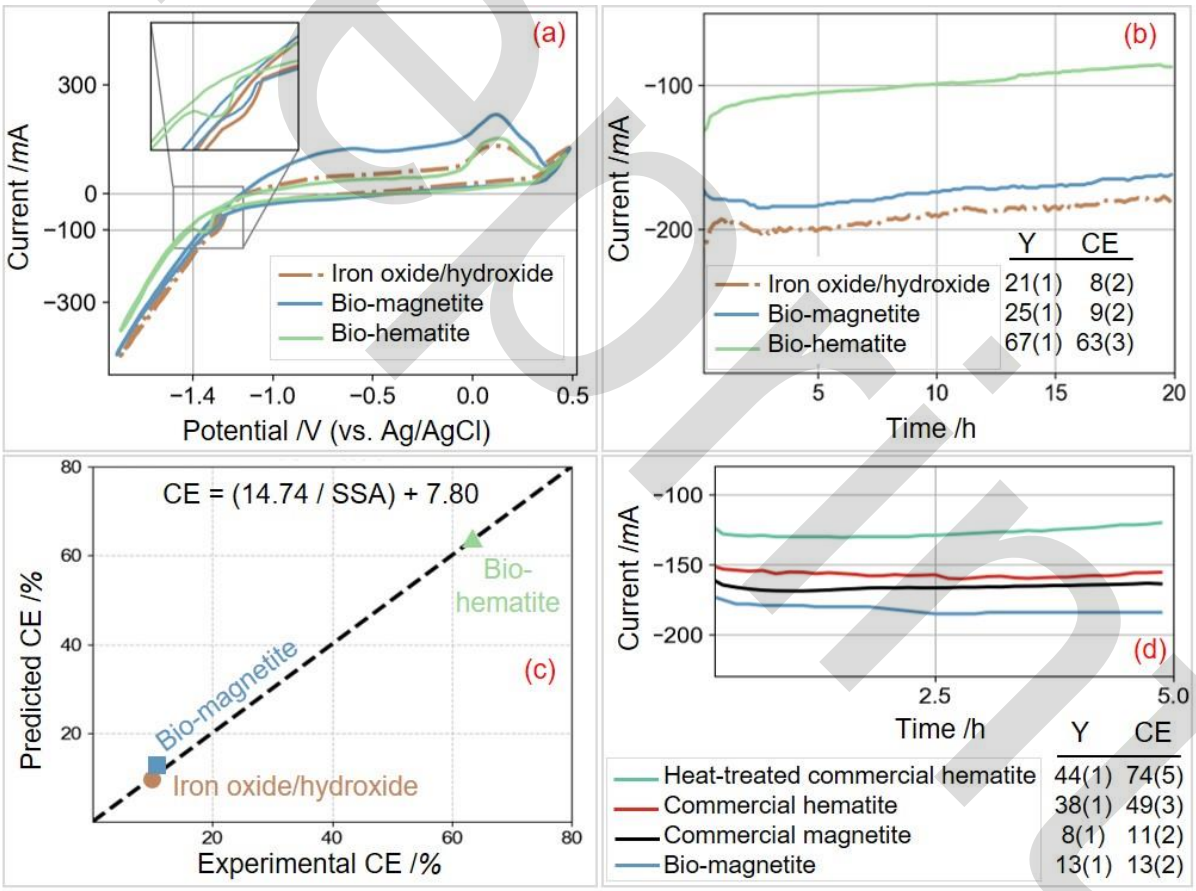

Figure 3. (a) The third cycle of cyclic voltammetry test and (b) the 20 h chronoamperometry result at -1.4 V vs. Ag/AgCl in 10 M NaOH for iron oxide/hydroxide as starting material, the biologically produced magnetite (bio-magnetite) and after heat treatment (bio-hematite) at 363 K and the obtained iron yields (Y) and current efficiencies (CE). (c) The parity plot presents a model for predicting the inverse correlation of current efficiency with specific surface area (SSA). (d) The comparison of reducibility of commercial hematite vs. that after

heat treatment, and commercial magnetite vs. bio-magnetite by 5 h electrolysis is shown as iron yield Y/wt.% and current efficiency CE/%. The numbers in brackets are the estimated standard deviations of the obtained values in the last digit. Note that the results of the 20 h tests (b) and the 5 h tests (d) are not directly comparable due to the different test durations. The former focuses on the main materials, while the latter are control tests on additional materials.

The bio-hematite currents remain relatively low and with minimal fluctuations throughout the electrolysis, with an extracted iron yield of 67(1) wt.%. This stability is indicative of a more steady and efficient iron electrochemical reduction process. In contrast, iron oxide/hydroxide (yield: 21(1) wt.%) and bio-magnetite (yield: 25(1) wt.%) exhibit higher currents and fluctuations despite lower yields, suggesting a lower selectivity and a less desired reduction process. These observations can be attributed to thermodynamic and microstructural factors.

Thermodynamically, the standard Gibs free energy, required for further electrochemical decomposition to elemental iron, reduces from 1013.7 kJ/mol for (Fe(II)/Fe(III)) oxides to 749.3 kJ/mol for Fe(III) oxides [48].

Furthermore, with its higher average crystallite size, bio-hematite provides a crystal structure with reduced micro-strain and bulk point defects that ensure pathways for electron movement that are more defined and less disrupted, which increases favorable iron reaction kinetics. The surface defects and morphology of iron oxide/hydroxide and bio-magnetite act as active sites for unwanted HER side reactions or inconsistent electron transfer. The higher SSA and the smaller ACS of iron oxide/hydroxide and bio-magnetite also mean greater surface-to-bulk volume, which increases the overall undesired electrochemical activity at the surface. Additionally, the dense magnetite shell causes lower diffusivity [49], supporting the formation of dense iron layers around the particle during the reduction, prohibiting further iron reduction as it was also shown for the reduction of iron oxides with hydrogen [50].

An inverse relationship between current efficiency (CE) and SSA for all three minerals is observable as shown in Supplementary (S5). The parity plot (Figure 3c) presents a model for predicting this correlation ($CE = 14.74 / SSA + 7.80$). The lower surface-to-bulk volume of bio-hematite means fewer active sites for parasitic HER and a more controlled contribution of electrons for iron reduction, with a high current efficiency of 63(3) %. In contrast, a higher surface area means more undesired electrochemical reactions as the efficiency decreases to 8(2) % for iron oxide/hydroxide and 9(2) % for bio-magnetite.

Zhang et al. [51] showed that nanostructured iron oxides as electrode materials present challenges such as low thermodynamic stability and susceptibility to surface side reactions. Pervez et al. [52] additionally showed that the crystalline phases of iron oxide nanotubes demonstrated superior electrochemical performance compared to their amorphous counterparts. This enhanced behavior was attributed to the better-crystallized part of a phase providing a more defined path for ion diffusion and electron transport, as evidenced by our results.

From a microstructural perspective, one might have anticipated that iron oxide/hydroxide would be much less efficient than bio-magnetite due to its SSA being about seven times higher. However, thermodynamics balances the scales, allowing more electrons to be dedicated to iron reduction. This is despite the abundance of active sites and side reactions. This is why iron oxide/hydroxide achieves a high yield and faradaic efficiency comparable to bio-magnetite.

The conversion of bio-hematite outperforms the other two materials in terms of iron yield, current efficiency, voltage efficiency, and energy consumption (Figure 4). The lower efficiency of non-heat-treated samples suggests that more electrical energy is diverted to non-productive processes. While bio-mining can act as a crucial upstream step in the extraction of iron oxide/hydroxides such as ferrihydrite from low-grade ore resources, intermediate oxidation using heat treatment is required to improve further electrochemical behavior.

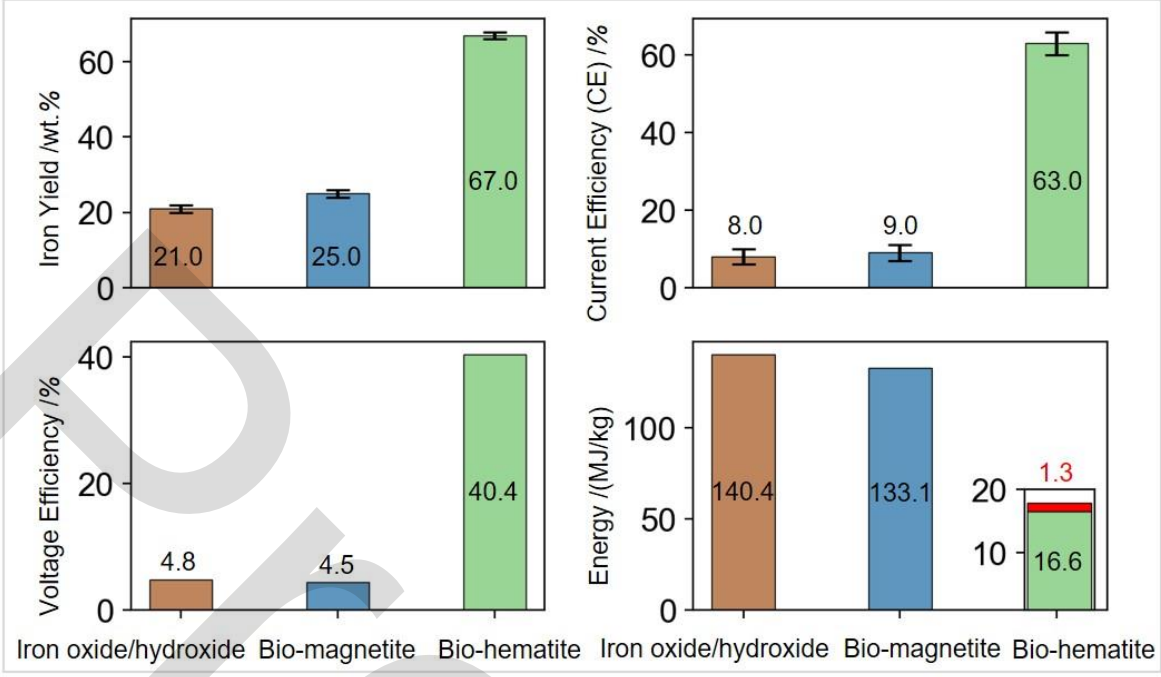

Figure 4. The values for iron extraction yield, current efficiency (CE), voltage efficiency, and energy consumption for iron oxide/hydroxide as the starting material, the biologically produced magnetite (bio-magnetite), and that after heat treatment (bio-hematite) after 20 h electrolysis at -1.4 V vs. Ag/AgCl in 10 M NaOH at 363 K. The error bars indicate the standard deviation. For bio-hematite, the required energy is divided into the energy for electrolysis (16.6 MJ/kg) and the additional energy for heating to 900 ℃ for heat treatment (1.3 MJ/kg).

In addition, bio-hematite requires a lower total cell voltage to maintain the applied cathodic potential, resulting in reduced electrolysis energy consumption and better voltage efficiency. Even considering the required energy capacity for heating up to 900 ℃ for thermal treatment, bio-hematite's total energy consumption is far less than that of iron oxide/hydroxide and bio-magnetite. For calculating this electrolysis energy consumption, the average cell voltage was multiplied by the electrical charge per mass of iron produced. The result is 17.9 MJ/kg, which is also lower than the estimated energy consumption of 19 MJ/kg for an industrial blast furnace [53]. We neglected bio-mining energy because *C. ferrireducens* can utilize in situ-produced H_2 from water electrolysis [41], making its energy input minimal compared to the electrolysis process.

The SEM images of the highly amorphous and scattered iron oxide/hydroxide vs. the smoother and more uniform surface with agglomerated particles of bio-magnetite confirm the microstructural changes caused by the bio-leaching process as the cellular components act as the nucleation points for crystallization (Figure 5). A further decrease in surface defects and increased agglomeration was achieved by the heat treatment process as it reduced surface irregularity and increased particle cohesion. In addition, the SEM image of a reduced bio-hematite after 20 hours of alkaline electrolysis shows areas where iron is inclusively present as individual phases. The elemental map data for Fe(0) is presented in Supplementary (S6).

While the recovered iron is not yet 100 % pure, the process is close to full conversion. The presence of minor impurities can be efficiently addressed through straightforward post-processing steps. Once these minor adjustments are made, the iron will be suitable for various applications, including construction, manufacturing, and space exploration. Addressing these challenges through additional processing steps will improve the material's quality, making it viable for broader industrial uses. These additional steps are common in metallurgy and do not

detract from the potential of the proposed process for sustainable iron production.

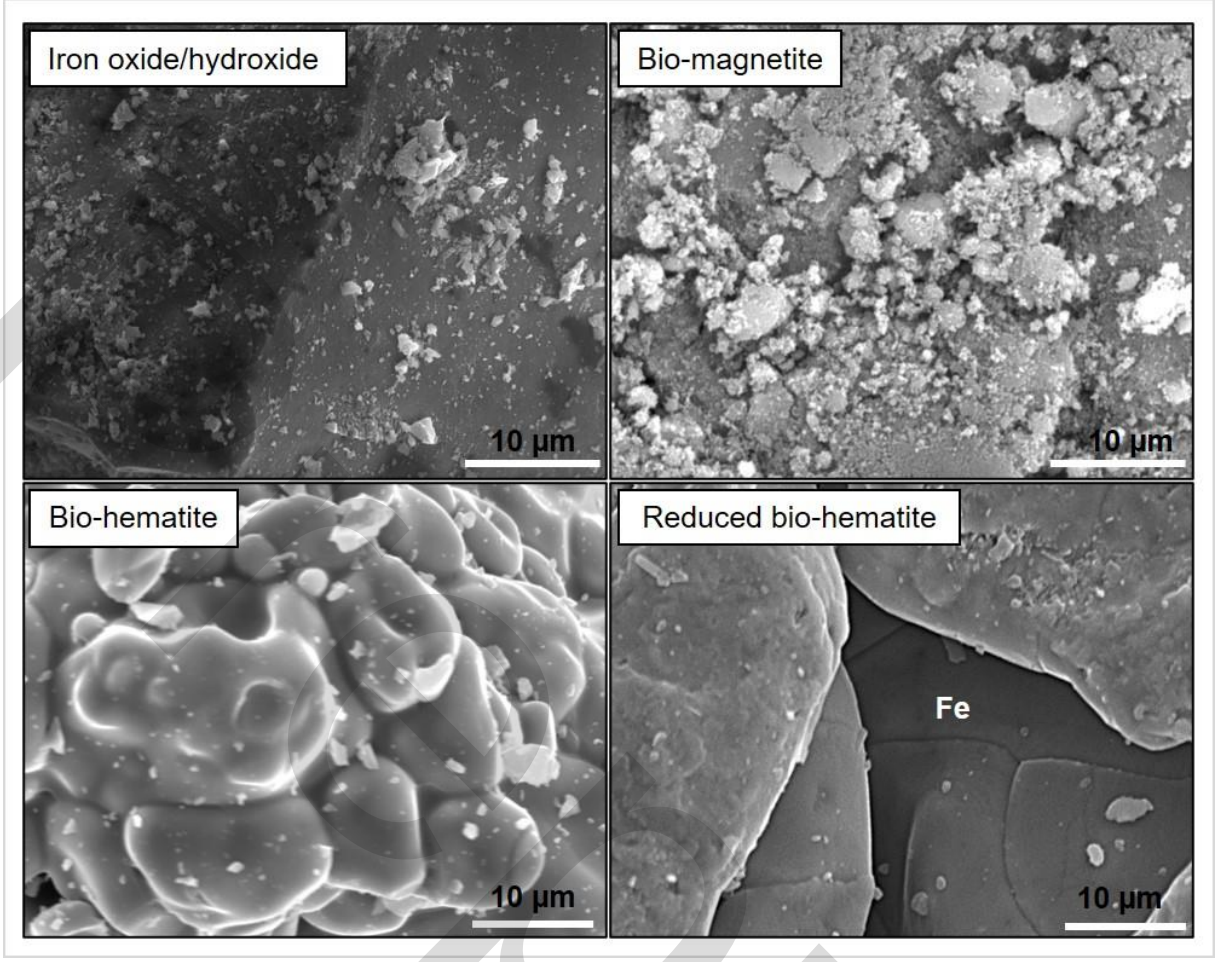

Figure 5. SEM images of iron oxide/hydroxide as the starting material, the biologically produced magnetite (bio-magnetite), and that after heat treatment (bio-hematite) confirm the microstructural changes during the bio-leaching and heat treatment processes. The image of a reduced bio-hematite after 20 h of electrolysis at -1.4 V vs. Ag/AgCl in 10 M NaOH at 363 K shows areas where Fe is inclusively present.

3.2. Effects of heat treatment and bio-mining

To cross-check heat treatment effects on microstructure and reducibility, control tests were conducted. Commercial hematite, with and without heat treatment, was subjected to alkaline electrolysis for 5 h. Commercial and biologically produced magnetite were also compared to gain a better insight into bio-leaching impacts. The electrolysis plots as well as the corresponding iron extraction yield and Faradaic efficiency are presented in Figure 3d. Note that these results are not directly comparable to the 20 h test results due to the different materials and test durations.

First, it can be seen that the reducibility of commercial hematite (both heat treated and untreated), with its single Fe(III) valence, outperforms commercial magnetite and bio-magnetite, as thermodynamically expected. The relatively less negative Gibbs free energy for these Fe(III) oxides as mentioned above suggests that under the same electrochemical conditions, they can be reduced to metallic iron more readily.

A comparative analysis of the microstructural properties of non-heat-treated commercial hematite (SSA: 2.6 m^2/g, DC: 95(5) %, ACS: 135(1) nm) and that after heat treatment (SSA: 0.76 m^2/g, DC: 99(5) %, ACS: 173(2) nm) confirms that thermal treatment results in a lower

specific surface area and higher ACS (Table 1). Electrochemically, the heat treatment of commercial hematite led to a decline in currents and a higher iron yield and current efficiency. This is further evidence of the influence of crystallinity and grain size on reducibility and side reactions. These observations, in line with the improvements noted in the previous section, corroborate the benefits of heat treatment optimizing iron oxide/hydroxide electrochemical properties.

We also observed a superior reducibility of bio-magnetite compared to a commercial magnetite. We compared commercial magnetite, with SSA of 8.1 m^2/g, DC of 87(5) %, and ACS of 74(1) nm, to bio-magnetite synthesized from the iron oxide/hydroxide in this research, with SSA of 41.5 m^2/g, a DC of 80(5) %, and ACS of 16.2(2) nm. Theoretically, the microstructural properties of commercial magnetite might be expected to confer advantages due to its lower SSA, suggesting fewer active sites and potentially reduced parasitic reactions. Despite this, our results indicated that bio-magnetite demonstrated enhanced electrochemical behavior in terms of iron yield and current efficiency.

EDX analysis revealed traces of carbon in the bio-magnetite sample (Supplementary S7), probably from decomposed microorganisms or the partial formation of siderite ($FeCO_3$). It is hypothesized that these organic residues could serve as binding sites to facilitate electron transfer, particularly enhancing iron reduction. The possible presence of siderite embedded within the bio-magnetite matrix could thermodynamically favor the reduction process. Previous studies suggest that the composition of the cultivation medium and specific parameters can influence mineral formation during bio-leaching, with siderite formation being reported in bicarbonate-buffered mediums like the one used in this research [54,55]. In particular, thermophilic iron-reducing microorganisms are known to produce mixtures of magnetite and siderite during the reduction of ferrihydrite [56]. Given the complexity of the bio-mineralization process, further studies are needed to confirm these findings fully.

4. Perspective

This research enabled us to identify a future approach for iron fabrication from low-grade iron resources such as the Martian regolith. The MGS-1 basaltic Mars regolith simulant is manufactured from a mixture of several rocks [57]. The composition consists of amorphous and crystalline phases. The composition list includes five iron-containing minerals, namely olivine, hematite, magnetite, ferrihydrite, and Fe-carbonate, as well as their iron contents (Table 2). It is evidence that ferrihydrite, the investigated mineral in this study, is the major iron-bearing phase of the Martian regolith.

Key challenges in extraterrestrial iron mining include the variable composition of Martian regolith and the limited availability of consistent energy sources. Martian regolith contains a mix of iron-bearing minerals, complicating extraction, while intermittent solar power requires efficient energy management [58].

Our attempt to reduce regolith directly using alkaline electrolysis at 363 K did not lead to any metal production as aqueous solutions do not provide a high enough potential window to decompose the complicated mixed mineral phases of regolith. Current methods, such as molten regolith electrolysis (~1873 K) and solid-state reduction (~1173 K), face significant challenges, including partial reductions, mixed metal outputs, incomplete oxygen removal, and unselective metal extraction, making them impractical for efficient use. To enable iron recovery using alkaline electrolysis at moderate temperatures, it is necessary to first precipitate the ferrous phases.

We, therefore, see the perspective that with an optimized upstream bio-mining beneficiation step, iron-containing phases could be converted to magnetically responsive forms. This property is crucial for isolating iron from the regolith's complex mixture of minerals. An intermediate heat treatment step before electrochemical reduction will also be suggested based on this study. The proposed concept for the fabrication of iron from Martian regolith is represented in Figure

6. This approach leverages ISRU, minimizing transport costs from Earth. Using Ni/Fe as a non-contaminating inert anode material also aligns with the nickel trace presence in Martian meteorites [59]. We underscore the importance of ongoing research to validate the concept for the MGS-1 Martian regolith simulant.

Table 2. The mineral composition (manufacturer fact sheet) of MGS-1 Martian regolith simulant and the iron content of the iron-bearing phases.

Mineral	Total /wt.%	Iron /wt.%
Crystalline		
Plagioclase	27.1	-
Pyroxene	20.3	-
Olivine	13.7	29.3
Hematite	0.5	5.1
Magnetite	1.9	20.3
Amorphous		
Anhydrite	1.7	-
Basaltic Glass	22.9	-
Hydrated Silica	3.0	-
Mg-sulfate	4.0	-
Ferrihydrite	3.5	35.4
Fe-carbonate	1.4	9.9

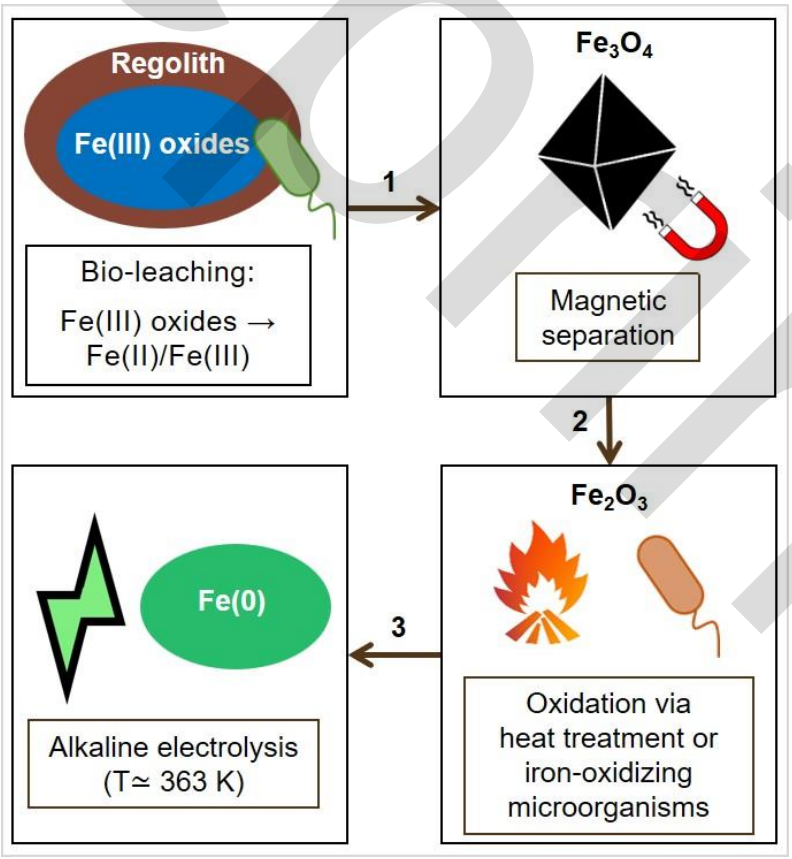

Figure 6. The proposed concept of alkaline deoxidation electrolysis with upstream bio-mining beneficiation and oxidation using thermal treating or iron-oxidizing microorganisms for extraterrestrial iron fabrication from Martian regolith.

Furthermore, further investigations are required to modify the proportion of microbial cells present in the bio-mined minerals as we showed that this may influence electrochemical behavior. Depending on the microbial species and the cultivation conditions, iron-reducing microorganisms may rely on different extracellular electron transfer mechanisms and strategies to reduce iron oxides, including direct contact with iron particles or electron shuttles (endogenous or exogenous) for iron reduction at a distance [60]. Likewise, the cultivation medium may include variable amounts of inorganic salts and organic matter, which might be bound to iron oxides [61].

Finally, microorganisms could also replace heat treatment. The idea would be to use iron-oxidizing microorganisms to bio-transform magnetite into ferric iron oxides such as hematite and maghemite or ferrous iron carbonate (siderite) [62,63,64]. This innovative combination could further decrease energy consumption as it could eliminate the heat treatment step which involves temperatures around 1173 K. Validation of the concept of bio-mining of Martian regolith to produce bio-magnetite, magnetic precipitation, and bio-oxidation (as a substitute for heat treatment) followed by alkaline electrolysis for iron production will be the subject of further studies.

5. Conclusion

This study addresses the challenges associated with the electrochemical reduction of low-grade iron ores by introducing bio-mineralization as a key beneficiation step. Ferrihydrite, a common iron-rich phase, was selected due to its abundance and potential for conversion. Through anaerobic respiration, iron-reducing bacteria convert ferrihydrite into bio-magnetite, allowing for magnetic separation of iron-bearing phases from impurities. This bio-magnetite was then successfully reduced to metallic iron via electrolysis in an alkaline medium at moderate temperatures. The inclusion of a heat treatment step further enhances the iron yield by converting bio-magnetite to bio-hematite, a phase that is thermodynamically easier to reduce. These findings provide a promising, sustainable pathway for iron production from low-grade resources, including potential applications in extraterrestrial environments like Mars, where conventional extraction methods are impractical.

Key takeaways from this work include:

1. Bio-Mineralization: Iron-reducing bacteria convert iron-bearing phases into bio-magnetite, enabling future magnetic separation and enrichment of iron in low-grade ores.
2. Electrochemical Reduction: Concentrated iron oxides were efficiently reduced to metallic iron using an energy-efficient electrochemical process in an alkaline medium.
3. Environmental Sustainability: This method offers a low-energy, low-emission alternative for extracting iron from waste and low-grade resources.
4. Extraterrestrial Application: The approach shows promise for iron extraction from Martian regolith, supporting future in-situ resource utilization for space missions.

The conversion of ferrihydrite to bio-magnetite, followed by its successful electrochemical reduction, achieved iron yields of 25(1) wt.% with a current efficiency of 9(2) % after 20 hours. Incorporating heat treatment increased the yield to 67(1) wt.% with a current efficiency of 63(3) %. Bio-hematite, with a simpler Fe(III) valence state, proved to be more reducible than bio-magnetite, reinforcing the benefits of heat treatment. Additionally, the estimated energy consumption of 17.9 MJ/kg is competitive with current industrial standards, demonstrating the viability of this approach.

This study also highlights the importance of microstructure on reducibility. Controlled heat

treatment improves crystallinity and reduces active sites for side reactions, such as hydrogen evolution while facilitating electron flow. However, excessive agglomeration could hinder electrolyte diffusion and oxygen ion release, underscoring the need for precise control of heat treatment parameters [65].
Looking ahead, while this study demonstrated promising short-term electrochemical stability, the long-term performance of the electrochemical reduction of bio-magnetite and bio-hematite under industrial conditions remains untested. Future work should prioritize validation of the concept for low-grade iron ores such as the Martian regolith simulant. Future efforts will then be required for scaling up, including the cultivation of iron-reducing bacteria, the management of bio-mineralization, and efficient by-product handling. Optimizing bioreactor systems, conducting comprehensive techno-economic analyses, and understanding the kinetics of iron reduction under varying operational conditions will be crucial for the commercial viability and industrial scalability of this process.

Data availability

All measurement data that are included in this publication are uploaded to an online repository [66] along with Python scripts to evaluate the data and generate the plots of this study.

Author contributions statement

R.F., F.L.M., M.B., A.C., G.P., S.K., and J.T. conceived the concept. R.F. conducted the electrochemical experiments and coordinated the overall workflow. F.L.M., M.B., and J.T. supervised the electrochemical part. A.C. performed the biological experiments. G.P. and S.K. supervised the biological work. Sample characterization was conducted by M.I.J.H. under the supervision of T.M.G. The manuscript was mainly written by R.F. All authors analyzed and discussed the results and revised the manuscript.

Funding

This project is part of the 'Humans on Mars Initiative' funded by the Federal State of Bremen and the University of Bremen.
For details on the projects refer to
Humans on Mars - Pathways to a long-term sustainable human presence
Learning from Mars to preserve Earth
https://www.uni-bremen.de/en/aerospace-at-the-university-of-bremen/humans-on-mars

Declaration of competing interest

The authors declare no competing interests.

Supporting information

The supplementary material is stored in a repository available at
https://doi.org/10.5281/zenodo.13283858

Correspondence and requests for materials should be addressed to J.T.

References

[1] A. Oarga-Mulec, U. Luin, M. Valant, Back to the future with emerging iron technologies, RSC Adv. (2024) 20765–20779. https://doi.org/10.1039/d4ra03565h.
[2] J. Kim, B.K. Sovacool, M. Bazilian, S. Griffiths, J. Lee, M. Yang, J. Lee, Decarbonizing the iron and steel industry: A systematic review of sociotechnical systems, technological innovations, and policy options, Energy Res. Soc. Sci. 89 (2022) 102565. https://doi.org/10.1016/j.erss.2022.102565.
[3] X. Wang, H. Yang, X. Yu, J. Hu, J. Cheng, H. Jing, Research progress in the preparation of iron by electrochemical reduction route without CO2 emissions, J. Appl.

Electrochem. 53 (2023) 1521–1536. https://doi.org/10.1007/s10800-023-01870-7.
[4] A. Ranzani, D. Wagner, F. Patisson, A. Ranzani, D. Wagner, F. Patisson, Modelling a new , low CO2 emissions , hydrogen steelmaking process To cite this version : HAL Id : hal-00943356 Modelling a new , low CO 2 emissions , (2014).
[5] R. Fayaz, I. Bösing, F. La Mantia, M. Baune, M.I.J. Hanafi, T.M. Gesing, J. Thöming, Deoxidation Electrolysis of Hematite in Alkaline Solution: Impact of Cell Configuration and Process Parameters on Reduction Efficiency, ChemElectroChem 10 (2023) 1–9. https://doi.org/10.1002/celc.202300451.
[6] M. Jovičević-Klug, I.R. Souza Filho, H. Springer, C. Adam, D. Raabe, Green steel from red mud through climate-neutral hydrogen plasma reduction, Nature 625 (2024) 703–709. https://doi.org/10.1038/s41586-023-06901-z.
[7] R.R. Wang, Y.Q. Zhao, A. Babich, D. Senk, X.Y. Fan, Hydrogen direct reduction (H-DR) in steel industry—An overview of challenges and opportunities, J. Clean. Prod. 329 (2021) 129797. https://doi.org/10.1016/j.jclepro.2021.129797.
[8] UN, Progress towards the Sustainable Development Goals, Report of the Secretary-General, Assembly 64782 (2024) 14.
[9] S.O. Ganiyu, C.A. Martínez-Huitle, The use of renewable energies driving electrochemical technologies for environmental applications, Curr. Opin. Electrochem. 22 (2020) 211–220. https://doi.org/10.1016/j.coelec.2020.07.007.
[10] M. Hecht, J. Hoffman, D. Rapp, J. McClean, J. SooHoo, R. Schaefer, A. Aboobaker, J. Mellstrom, J. Hartvigsen, F. Meyen, E. Hinterman, G. Voecks, A. Liu, M. Nasr, J. Lewis, J. Johnson, C. Guernsey, J. Swoboda, C. Eckert, C. Alcalde, M. Poirier, P. Khopkar, S. Elangovan, M. Madsen, P. Smith, C. Graves, G. Sanders, K. Araghi, M. de la Torre Juarez, D. Larsen, J. Agui, A. Burns, K. Lackner, R. Nielsen, T. Pike, B. Tata, K. Wilson, T. Brown, T. Disarro, R. Morris, R. Schaefer, R. Steinkraus, R. Surampudi, T. Werne, A. Ponce, Mars Oxygen ISRU Experiment (MOXIE), Space Sci. Rev. 217 (2021). https://doi.org/10.1007/s11214-020-00782-8.
[11] C.W. Childs, Ferrihydrite: A review of structure, properties and occurrence in relation to soils, Soil Conserv. (1992).
[12] J. Filip, R. Zboril, O. Schneeweiss, J. Zeman, M. Cernik, P. Kvapil, M. Otyepka, Environmental applications of chemically pure natural ferrihydrite, Environ. Sci. Technol. 41 (2007) 4367–4374. https://doi.org/10.1021/es062312t.
[13] D.A. Bazylinski, R.B. Frankel, K.O. Konhauser, Modes of biomineralization of magnetite by microbes, Geomicrobiol. J. 24 (2007) 465–475. https://doi.org/10.1080/01490450701572259.
[14] B.L. Ehlmann, C.S. Edwards, Mineralogy of the Martian surface, Annu. Rev. Earth Planet. Sci. 42 (2014) 291–315. https://doi.org/10.1146/annurev-earth-060313-055024.
[15] E. Hinterman, Simulating oxygen production on Mars for the Mars Oxygen In-Situ Resource Utilization Experiment, Acta Astronaut. 170 (2020) 678–685. https://doi.org/10.1016/j.actaastro.2020.02.043.
[16] L. Schlüter, A. Cowley, Review of techniques for In-Situ oxygen extraction on the moon, Planet. Space Sci. 181 (2020) 104753. https://doi.org/10.1016/j.pss.2019.104753.
[17] M.S. Humbert, G.A. Brooks, A.R. Duffy, C. Hargrave, M.A. Rhamdhani, Thermophysical property evolution during molten regolith electrolysis, Planet. Space Sci. 219 (2022) 105527. https://doi.org/10.1016/j.pss.2022.105527.
[18] S.S. Schreiner, L. Sibille, J.A. Dominguez, J.A. Hoffman, A parametric sizing model for Molten Regolith Electrolysis reactors to produce oxygen on the Moon, Adv. Sp. Res. 57 (2016) 1585–1603. https://doi.org/10.1016/j.asr.2016.01.006.
[19] A. Meurisse, B. Lomax, Á. Selmeci, M. Conti, R. Lindner, A. Makaya, M.D. Symes, J. Carpenter, Lower temperature electrochemical reduction of lunar regolith simulants in

molten salts, Planet. Space Sci. 211 (2022). https://doi.org/10.1016/j.pss.2021.105408.
[20] I. Bösing, F. La Mantia, J. Thöming, Modeling of electrochemical oxide film growth-a PDM refinement, Electrochim. Acta 406 (2022). https://doi.org/10.1016/j.electacta.2022.139847.
[21] J.F. Monteiro, Y.A. Ivanova, A. V. Kovalevsky, D.K. Ivanou, J.R. Frade, Reduction of magnetite to metallic iron in strong alkaline medium, Electrochim. Acta 193 (2016) 284–292. https://doi.org/10.1016/j.electacta.2016.02.058.
[22] V. Feynerol, H. Lavelaine, P. Marlier, M.N. Pons, F. Lapicque, Reactivity of suspended iron oxide particles in low temperature alkaline electrolysis, J. Appl. Electrochem. 47 (2017) 1339–1350. https://doi.org/10.1007/s10800-017-1127-5.
[23] D. V. Lopes, A.D. Lisenkov, S.A. Sergiienko, G. Constantinescu, A. Sarabando, M.J. Quina, J.R. Frade, A. V. Kovalevsky, Alkaline Electrochemical Reduction of a Magnesium Ferrospinel into Metallic Iron for the Valorisation of Magnetite-Based Metallurgical Waste, J. Electrochem. Soc. 168 (2021) 073504. https://doi.org/10.1149/1945-7111/ac1490.
[24] A. Maihatchi, M.N. Pons, Q. Ricoux, F. Goettmann, F. Lapicque, Electrolytic iron production from alkaline suspensions of solid oxides: Compared cases of hematite, iron ore and iron-rich bayer process residues, J. Electrochem. Sci. Eng. 10 (2020) 95–102. https://doi.org/10.5599/jese.751.
[25] D. V. Lopes, A.D. Lisenkov, L.C.M. Ruivo, A.A. Yaremchenko, J.R. Frade, . A. V. Kovalevsky, Prospects of Using Pseudobrookite as an Iron-Bearing Mineral for the Alkaline Electrolytic Production of Iron, Materials (Basel). 15 (2022) 1–19. https://doi.org/10.3390/ma15041440.
[26] D.B. Johnson, Biomining-biotechnologies for extracting and recovering metals from ores and waste materials, Curr. Opin. Biotechnol. 30 (2014) 24–31. https://doi.org/10.1016/j.copbio.2014.04.008.
[27] Y. Gumulya, L. Zea, A.H. Kaksonen, In situ resource utilisation: The potential for space biomining, Miner. Eng. 176 (2022) 107288. https://doi.org/10.1016/j.mineng.2021.107288.
[28] C.S. Cockell, R. Santomartino, K. Finster, A.C. Waajen, L.J. Eades, R. Moeller, P. Rettberg, F.M. Fuchs, R. Van Houdt, N. Leys, I. Coninx, J. Hatton, L. Parmitano, J. Krause, A. Koehler, N. Caplin, L. Zuijderduijn, A. Mariani, S.S. Pellari, F. Carubia, G. Luciani, M. Balsamo, V. Zolesi, N. Nicholson, C.M. Loudon, J. Doswald-Winkler, M. Herová, B. Rattenbacher, J. Wadsworth, R. Craig Everroad, R. Demets, Space station biomining experiment demonstrates rare earth element extraction in microgravity and Mars gravity, Nat. Commun. 11 (2020) 1–11. https://doi.org/10.1038/s41467-020-19276-w.
[29] R. Volger, G.M. Pettersson, S.J.J. Brouns, L.J. Rothschild, A. Cowley, B.A.E. Lehner, Mining moon & mars with microbes: Biological approaches to extract iron from Lunar and Martian regolith, Planet. Space Sci. 184 (2020) 104850. https://doi.org/10.1016/j.pss.2020.104850.
[30] S.M. Castelein, T.F. Aarts, J. Schleppi, R. Hendrikx, A.J. Böttger, D. Benz, M. Marechal, A. Makaya, S.J.J. Brouns, M. Schwentenwein, A.S. Meyer, B.A.E. Lehner, Iron can be microbially extracted from Lunar and Martian regolith simulants and 3D printed into tough structural materials, PLoS One 16 (2021) 1–21. https://doi.org/10.1371/journal.pone.0249962.
[31] E. Viollier, P.W. Inglett, K. Hunter, A.N. Roychoudhury, P. Van Cappellen, The Ferrozine method revisted, Appl. Geochemistry 15 (2000) 785–790.
[32] S. lan Wang, G.M. Haarberg, E. Kvalheim, Electrochemical Behavior of Dissolved Fe2O3 in Molten CaCl2-KF, J. Iron Steel Res. Int. 15 (2008) 48–51. https://doi.org/10.1016/S1006-706X(08)60265-4.

[33] L. Trotochaud, S.L. Young, J.K. Ranney, S.W. Boettcher, Nickel-Iron oxyhydroxide oxygen-evolution electrocatalysts: The role of intentional and incidental iron incorporation, J. Am. Chem. Soc. 136 (2014) 6744–6753. https://doi.org/10.1021/ja502379c.
[34] D.J.S. Hyslop, A.M. Abdelkader, A. Cox, D.J. Fray, Utilization of Constant Current Chronopotentiometry to Synthesize a Co–Cr Alloy, J. Electrochem. Soc. 157 (2010) E111. https://doi.org/10.1149/1.3427511.
[35] J. Qiao, Y. Liu, F. Hong, J. Zhang, A review of catalysts for the electroreduction of carbon dioxide to produce low-carbon fuels, Chem. Soc. Rev. 43 (2014) 631–675. https://doi.org/10.1039/c3cs60323g.
[36] T.M. Gesing, L. Robben, Determination of the average crystallite size and the crystallite size distribution: The envelope function approach EnvACS., J. Appl. Crystallogr. (2024). https://doi.org/10.1107/S1600576724007362.
[37] A. Slobodkin, A.L. Reysenbach, N. Strutz, M. Dreier, J. Wiegel, Thermoterrabacterium ferrireducens gen. nov., sp. nov., a thermophilic anaerobic dissimilatory Fe(III)-reducing bacterium from a continental hot spring, Int. J. Syst. Bacteriol. 47 (1997) 541–547. https://doi.org/10.1099/00207713-47-2-541.
[38] S.N. Gavrilov, D.G. Zavarzina, I.M. Elizarov, T. V. Tikhonova, N.I. Dergousova, V.O. Popov, J.R. Lloyd, D. Knight, M.Y. El-Naggar, S. Pirbadian, K.M. Leung, F.T. Robb, M. V. Zakhartsev, O. Bretschger, E.A. Bonch-Osmolovskaya, Novel Extracellular Electron Transfer Channels in a Gram-Positive Thermophilic Bacterium, Front. Microbiol. 11 (2021) 1–21. https://doi.org/10.3389/fmicb.2020.597818.
[39] C. Verseux, M. Baqué, K. Lehto, J.P.P. De Vera, L.J. Rothschild, D. Billi, Sustainable life support on Mars - The potential roles of cyanobacteria, Int. J. Astrobiol. 15 (2016) 65–92. https://doi.org/10.1017/S147355041500021X.
[40] C. Verseux, C. Heinicke, T.P. Ramalho, J. Determann, M. Duckhorn, M. Smagin, M. Avila, A Low-Pressure, N2/CO2 Atmosphere Is Suitable for Cyanobacterium-Based Life-Support Systems on Mars, Front. Microbiol. 12 (2021) 1–15. https://doi.org/10.3389/fmicb.2021.611798.
[41] S.N. Gavrilov, E.A. Bonch-Osmolovskaya, A.I. Slobodkin, Physiology of organotrophic and lithotrophic growth of the thermophilic iron-reducing bacteria Thermoterrabacterium ferrireducens and Thermoanaerobacter siderophilus, Microbiology 72 (2003) 132–137. https://doi.org/10.1023/A:1023299410478.
[42] A.I. Slobodkin, Thermophilic microbial metal reduction, Mikrobiologiya 74 (2005) 581–595.
[43] V. Vandieken, M. Mußmann, H. Niemann, B.B. Jørgensen, Desulfuromonas svalbardensis sp. nov. and Desulfuromusa ferrireducens sp. nov., psychrophilic, Fe(III)-reducing bacteria isolated from Arctic sediments, Svalbard, Int. J. Syst. Evol. Microbiol. 56 (2006) 1133–1139. https://doi.org/10.1099/ijs.0.63639-0.
[44] K. Kashefi, D.R. Lovley, Extending the upper temperature limit for life, Science (80-.). 301 (2003) 934. https://doi.org/10.1126/science.1086823.
[45] T.J. Beveridge, R.G.E. Murray, Sites of metal deposition in the cell wall of Bacillus subtilis, J. Bacteriol. 141 (1980) 876–887. https://doi.org/10.1128/jb.141.2.876-887.1980.
[46] J.B. Fein, Quantifying the effects of bacteria on adsorption reactions in water-rock systems, Chem. Geol. 169 (2000) 265–280. https://doi.org/10.1016/S0009-2541(00)00207-2.
[47] M.M. Sk, P. Pradhan, B.K. Patra, A.K. Guria, Green biomass derived porous carbon materials for electrical double-layer capacitors (EDLCs), Mater. Today Chem. 30 (2023). https://doi.org/10.1016/j.mtchem.2023.101582.
[48] D.W. Green, R.H. Perry, Perry's Chemical Engineers' Handbook, Eighth Edi,

McGraw-Hill, 2008.
https://www.accessengineeringlibrary.com/content/book/9780071422949.
[49] A. Heidari, N. Niknahad, M. Iljana, T. Fabritius, A review on the kinetics of iron ore reduction by hydrogen, Materials (Basel). 14 (2021). https://doi.org/10.3390/ma14247540.
[50] D. Spreitzer, J. Schenk, Reduction of Iron Oxides with Hydrogen—A Review, Steel Res. Int. 90 (2019). https://doi.org/10.1002/srin.201900108.
[51] L. Zhang, H. Bin Wu, X.W. Lou, Iron-oxide-based advanced anode materials for lithium-ion batteries, Adv. Energy Mater. 4 (2014) 1–11. https://doi.org/10.1002/aenm.201300958.
[52] S.A. Pervez, D. Kim, U. Farooq, A. Yaqub, J.H. Choi, Y.J. Lee, C.H. Doh, Comparative electrochemical analysis of crystalline and amorphous anodized iron oxide nanotube layers as negative electrode for LIB, ACS Appl. Mater. Interfaces 6 (2014) 11219–11224. https://doi.org/10.1021/am501370f.
[53] H.Y. Sohn, Y. Mohassab, Greenhouse Gas Emissions and Energy Consumption of Ironmaking Processes, 2016. https://doi.org/https://doi.org/10.1007/978-3-319-39529-6_25.
[54] J.M. Zachara, R.K. Kukkadapu, J.K. Fredrickson, Y.A. Gorby, S.C. Smith, Biomineralization of poorly crystalline Fe(III) oxides by dissimilatory metal reducing bacteria (DMRB), Geomicrobiol. J. 19 (2002) 179–207. https://doi.org/10.1080/01490450252864271.
[55] H. Dong, J.K. Fredrickson, D.W. Kennedy, J.M. Zachara, R.K. Kukkadapu, T.C. Onstott, Mineral transformation associated with the microbial reduction of magnetite, Chem. Geol. 169 (2000) 299–318. https://doi.org/10.1016/S0009-2541(00)00210-2.
[56] A. Piepenbrock, U. Dippon, K. Porsch, E. Appel, A. Kappler, Dependence of microbial magnetite formation on humic substance and ferrihydrite concentrations, Geochim. Cosmochim. Acta 75 (2011) 6844–6858. https://doi.org/10.1016/j.gca.2011.09.007.
[57] K.M. Cannon, D.T. Britt, T.M. Smith, R.F. Fritsche, D. Batcheldor, Mars global simulant MGS-1: A Rocknest-based open standard for basaltic martian regolith simulants, Icarus 317 (2019) 470–478. https://doi.org/10.1016/j.icarus.2018.08.019.
[58] S.O. Ganiyu, C.A. Martínez-Huitle, M.A. Rodrigo, Renewable energies driven electrochemical wastewater/soil decontamination technologies: A critical review of fundamental concepts and applications, Appl. Catal. B Environ. 270 (2020) 118857. https://doi.org/10.1016/j.apcatb.2020.118857.
[59] P. Kong, M. Ebihara, H. Palme, Siderophile elements in Martian meteorites and implications for core formation in Mars, Geochim. Cosmochim. Acta 63 (1999) 1865–1875. https://doi.org/10.1016/S0016-7037(99)00030-7.
[60] K.P. Nevin, D.R. Lovley, Mechanisms for Fe(III) oxide reduction in sedimentary environments, Geomicrobiol. J. 19 (2002) 141–159. https://doi.org/10.1080/01490450252864253.
[61] R.M. Cornell, U. Schwertmann, Adsorption of Ions and Molecules, 2003. https://doi.org/10.1002/3527602097.ch11.
[62] K.A. Weber, L.A. Achenbach, J.D. Coates, Microorganisms pumping iron: Anaerobic microbial iron oxidation and reduction, Nat. Rev. Microbiol. 4 (2006) 752–764. https://doi.org/10.1038/nrmicro1490.
[63] D. Brown A.*, B. Sherrif L., J. Sawicki A., Microbial transformation of magnetite to hematite, Geochim. Cosmochim. Acta 61 (1997) 3341–3348.
[64] L.O. Ohenhen, J.M. Feinberg, L.D. Slater, D. Ntarlagiannis, I.M. Cozzarelli, M. Rios-Sanchez, C.W. Isaacson, A. Stricker, E.A. Atekwana, Microbially Induced Anaerobic Oxidation of Magnetite to Maghemite in a Hydrocarbon-Contaminated Aquifer, J. Geophys. Res. Biogeosciences 127 (2022) 1–24.

https://doi.org/10.1029/2021JG006560.
[65] G.Z. Chen, E. Gordo, D.J. Fray, Direct electrolytic preparation of chromium powder, Metall. Mater. Trans. B Process Metall. Mater. Process. Sci. 35 (2004) 223–233. https://doi.org/10.1007/s11663-004-0024-6.
[66] R. Fayaz, (2024). Data Availability. Zenodo. https://doi.org/10.5281/zenodo.13284391